AIMS Energy, 10(1): 149–176.
DOI: 10.3934/energy.2022009
Received: 25 January 2022
Revised: 16 March 2022
Accepted: 23 March 2022
Published: 28 March 2022

http://www.aimspress.com/journal/energy

Review

Recent advances in polymer structures for organic solar cells: A review

Taihana Paula and Maria de Fatima Marques*

Instituto de Macromoléculas Professora Eloisa Mano—Universidade Federal do Rio de Janeiro, Av. Horácio Macedo, 2.030, Centro de Tecnologia, Bloco J, Cidade Universitária, CEP 21941-598-Rio de Janeiro, RJ, Brazil

* **Correspondence:** Email: fmarques@ima.ufrj.br; Tel: +552139387220.

Abstract: High energy dependence on fossil fuels and an increase in greenhouse gas emissions are factors that highlight the need for alternative energy sources. Photovoltaic technology is a strong candidate that uses the most abundant resource, solar energy, but what makes its wide use difficult is the high cost of the commercially available devices. Thus, research has been devoted to developing new low-cost photovoltaic systems that are easier to manufacture with high efficiency and durability, such as the third-generation solar cells. According to this study, organic solar cells (OPV) with polymers in the active layers are more prominent concerning power conversion efficiency associated with durability, resulting in great research interest. Furthermore, polymer solar cells are easier to process and can be manufactured on a large scale achieving high efficiencies and stability. This review aims to raise the state of the art about these solar cells, discourse their architectures, current developments on polymer structures, and most relevant challenges for OPV devices, as a search for increased efficiency and stability.

Keywords: conjugated polymers; polymeric semiconductors; photovoltaic devices; organic solar cells

1. Introduction

The third-generation solar cells are a class that emerged from the attempt to lower the cost of photovoltaic technology, improve large-scale production due to better processability, and use more abundant materials [1]. Among the types of photovoltaic systems in this class of solar cells, devices that contain an organic semiconductor (OSC) in the active layer stand out. This type of system makes

up the so-called organic solar cells (or organic photovoltaics, OPV). The initial attempt to obtain an OPV device used anthracene crystals as an energy conversion material [2]. In the beginning, OPVs were developed using structures of bilayer devices (small molecule (SM)/fullerene), achieving a power conversion efficiency (PCE) of 0.9%. After that, great attention came to the possibility of processing the main layer of OPV in solution due to the advantages in allowing the manufacture of flexible and lightweight solar panels through low-cost printing technologies, with the possibility of large-scale production [3–5]. It is especially the case of using conjugated polymers in the active layer due to the ease of polymeric materials to form good quality films with nanometric thickness. Therefore, the photoactive layer comprises polymeric semiconductors to form large, homogenous, smooth films. In this case, OPV is called a plastic solar cell. Moreover, the substrate can be made of a plastic film, such as poly(ethylene terephthalate) PET, instead of glass, which makes the solar panels flexible and light.

The polymers initially applied in OPV were poly[2-methoxy-5-(2'-ethyl-hexyloxy)-1,4-phenylene-vinylene] (MEH-PPV), poly[2-methoxy-5-(3',7′-dimethyl octyloxy)-1,4-phenylenevinylene) (MDMO-PPV), and other PPV-based materials. However, the efficiency did not exceed 3% because the wide bandgap of these polymers (above 1.9 eV) did not allow effective photon collection, which significantly limited the additional optimization of the device's performance. Polythiophenes and, especially, poly[3-hexylthiophene-2,5-diyl] (P3HT) were highlighted, achieving performances of 5% [6]. These results motivated the development of increasingly advanced technologies to improve solar cells, which still have numerous challenges that include increasing the efficiency and the durability of these devices [7].

The efficiency of OPV has been considerably improved with the synthesis of soluble fullerene derivatives and the development of bulk heterojunction (BHJ) active layers. In this case, the electron donor polymer (D) and the electron acceptor material (A), the modified fullerene, are dissolved in the same solution. Then, the film is processed directly from this solution, resulting in an active film with multiple D/A interfaces, analogous to the p-n interfaces in traditional semiconductors, where electric charges are generated after photoexcitation [8,9]. Therefore, the active BHJ-type layer corresponds to a film of a mixture of two organic materials. The first is a conjugated polymer that absorbs the light, produces the excitons, diffuses them to the p-n junction, and acts as an electron donor capable of transporting positive charges (holes) to the anode (p-OSC). An electron acceptor (n-OSC) will transport the electrons to the electrode (cathode). These two phases build an interpenetrating network, providing a 3D structure that enhances the diffusion of excitons and the transfer of charges [7].

A wide variety of conjugated polymers has been studied as a photoactive donor material in organic photovoltaic energy (OPVs), showing conversion efficiencies (PCEs) greater than 10% [11–15], which has further stimulated the development of organic solar cells. However, after 2015, the efficiencies of organic photovoltaic cells have risen sharply to values above 13%, currently reaching PCE greater than 18%. It occurred with the emergence of electron acceptor materials replacing fullerene, the non-fullerene acceptors (NFAs); some of them are also polymers (n-semiconductors) [16–18].

To better comprehend the influence of polymeric material on an OPV device, it is necessary to understand how these devices work and their architecture, themes that will be arranged in the following sections.

2. OPV operation mechanism

Unlike a conventional inorganic semiconductor, in which optical absorption immediately generates free charges, in organic semiconductors, optical absorption leads to the excitation of the electron donor polymer present in the active layer. As a result, this electron must at least overcome the energy of the bandgap (Eg, the difference between the LUMO and HOMO energies), which corresponds to the energetic leap from the occupied molecular orbital of higher energy (HOMO) to the lower energy unoccupied molecular orbital (LUMO), resulting in the formation of a spatially located electron-hole pair (exciton) attracted by Coulomb's electrostatic force (Figure 1) [18].

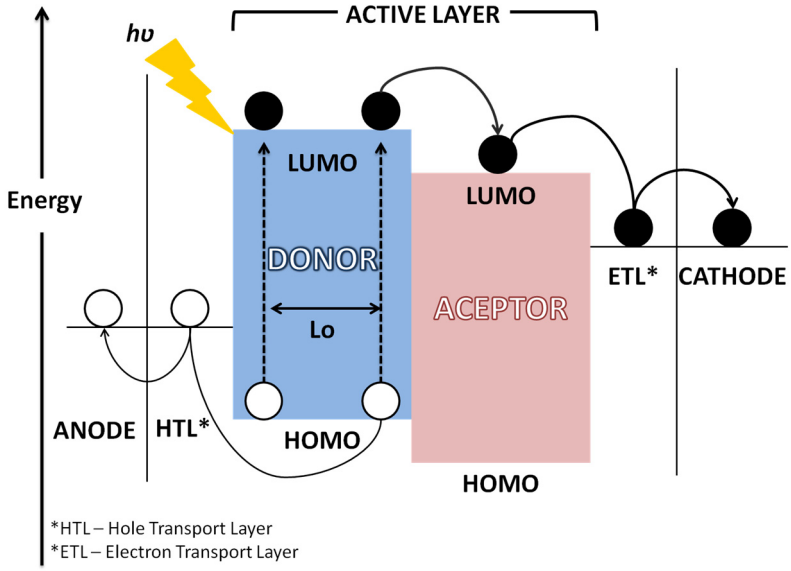

Figure 1. Mechanism for converting photons to electric charges in organic photovoltaic cells (OPV). Adapted from [18].

For the solar cell to generate electrical output, the excitons must diffuse to the donor-acceptor interface of the active layer. Its dissociation will occur and result in the appearance of holes in the donor component (p-type semiconductor) and electrons in the acceptor (n-type semiconductor). Finally, the charge carriers are taken to the respective electrodes with the aid of the internal electric field resulting from the difference in the working function of the electrodes. Thus, the generation of the photocurrent occurs [7]. For active layers of OPV-BHJ, several critical factors such as absorption profiles, energy level alignment, charge carrier mobility, and donor and acceptor materials' miscibility should be carefully considered [19,20].

The performance of an OPV device is reflected in three photovoltaic parameters: short circuit current density (J_{SC}), open-circuit voltage (V_{OC}), and fill factor (FF), and from these parameters, the power conversion efficiency (PCE, in percentage) can be calculated, which is directly proportional to those parameters. J_{SC} (mA/cm^2) is the density of current that flows through the external circuit when the cell electrodes are short-circuited (voltage = 0). It is proportional to the number of photons absorbed; it depends on the intensity and absorption range of the active layer materials. It can be enhanced using low Eg conjugated polymers, improving the D/A phase separation, and using materials with high light absorption. V_{OC} (V) corresponds to the electrical potential difference

between the two terminals of the device when disconnected from any circuit (J = 0). The voltage compensates for the current flow through the external circuit. It is related to the miscibility of the materials in the active layer. Also, it depends on the difference between the HOMO energy of the polymer donor and the LUMO of the acceptor and on the difference between the work function of the electrodes. J_{SC} is related to efficient light collection and the generation and carriers mobility.

Thus, a high J_{SC} can also be achieved by selecting materials with absorption spectra that overlap with the photon flux density and, therefore, the Sun incident power spectrum [21,22]. In this regard, molecular orbital levels, absorption coefficients, layer morphology, and molecular diffusion length are the main factors that control the final result [23]. Incompatible power levels resulted in low FF and lower device efficiency [24]. The fill factor FF is the ratio between the maximum power (P_{max} = J.V at the maximum power) generated by a cell and the product of V_{OC} x J_{SC}. FF is the 'square' of the current-voltage (J-V) curve and represents how hard or easy photogenerated carriers can be extracted from a photovoltaic device. It is one of the most significant and sensitive parameters in solar cells' characterization. It contains information from all processes involved in transporting, collecting, and recombining charges [25,26]. Losses of photocurrent can occur due to the recombination of electrons and holes; therefore, FF is an index that translates the loss of energy generation.

For electron donor polymers, a low Eg is desirable, and a lower HOMO energy level contributes to the increase in the V_{OC} of the device. However, V_{OC} is not only affected by the constituent materials of the active layer. For example, suboptimal contacts can lead to resistive losses—serial resistances that must be minimal; and shunt current—parallel resistance, which has to be maximal, causes a voltage drop. Therefore, device engineering and solar cell layout are important to ensure a high V_{OC} [27].

It is still a great challenge to find optimal pairs of donor-acceptors with complementary absorption, properly combined molecular orbital boundary levels, and well-mixed nanoscale morphology with crystalline self-organization in each domain to facilitate favorable generation and transport photocurrents [28]. In addition to the absorption and energy levels of the D/A pairs, the miscibility and morphology of the active layer is another critical factor that affects photovoltaic performance [29,30]. It takes many D/A interfaces to dissociate more excitons and increase the photocurrent. At the same time, the size of the domains of each phase of the material and its interconnection is important to optimize charge transport and minimize the recombination rate [31,32]. In addition to intrinsic characteristics of the D/A materials chosen, morphology, compatibility, and processing also have a strong influence on the efficiency of the device, which can be improved through some strategies, with the use of additives, annealing techniques, alternatives that can increase the extraction and transport of charge, along with a better morphology and molecular crystallinity.

Another important variable in the study of OPV is the thickness of the active layer. As the device thickness increases, the J_{SC} increases, the V_{OC} remains the same; however, the FF decreases. Therefore, increasing the active layer's thickness will lengthen the light absorption path and improve light capture within the device; however, this could ruin the charge transport properties [33].

Finally, the device's optimal performance is a confluence of increased J_{SC} and decreased FF. This characteristic behavior is caused by the low mobility of organic semiconductor carriers. Despite alternative manufacturing/processing procedures, the insertion of buffer layers (between the active layer and the electrodes, namely hole and electron transport layers, HTL and ETL) for a better combination of energy levels has been an exploited way to improve contact selectivity and device

rectification, resulting in an improved FF, usually measured as a consequence of modifying the device architectures [34].

3. OPV architecture

Polymeric devices are usually formed by several nanometric layers deposited on a substrate, such as glass, or a flexible substrate like poly(ethylene terephthalate) PET. Significant efforts have been made to improve the efficiency of OPV cells by introducing new buffer layers to reduce roughness improving adhesion between layers, and obtaining efficient extraction of charges from the molecular orbitals in the active layer materials [35].

Currently, the conventional architecture of OPV (Figure 2a) is formed by at least five components: i) transparent layer of indium and tin oxide (ITO) as a hole collection electrode (anode); ii) hole transport layer (HTL), where the injection of holes and electron blocking occurs; iii) the active layer, consisting of conjugated electron donor polymer (e^-), mixed with an electron-acceptor material, derived from fullerene or another n-type semiconductor, usually in the mass ratio of 1:1 [4]; iv) electron transport layer (ETL), such as Ca or LiF, to adjust the energy level; and v) metal electrode of low working function (Al, Ca/Al), as a cathode, the electron collector [36]. In this case, the most used material as HTL in conventional architecture is the mixture of ionomers consisting of poly(3,4-ethylenedioxythiophene):poly(styrene sulfonate), PEDOT:PSS, due to its compatibility function with ITO and excellent adjustment at the energy level [4]. The most traditional active layer is composed of poly(3-hexylthiophene) (P3HT) along with an organophilic fullerene ($C_{x)}$:acid methyl ester(6.6)-phenyl-C61-butyric (PCBM), such as $PC_{61}BM$, or a fullerene with a larger structure as the $PC_{71}BM$ [37].

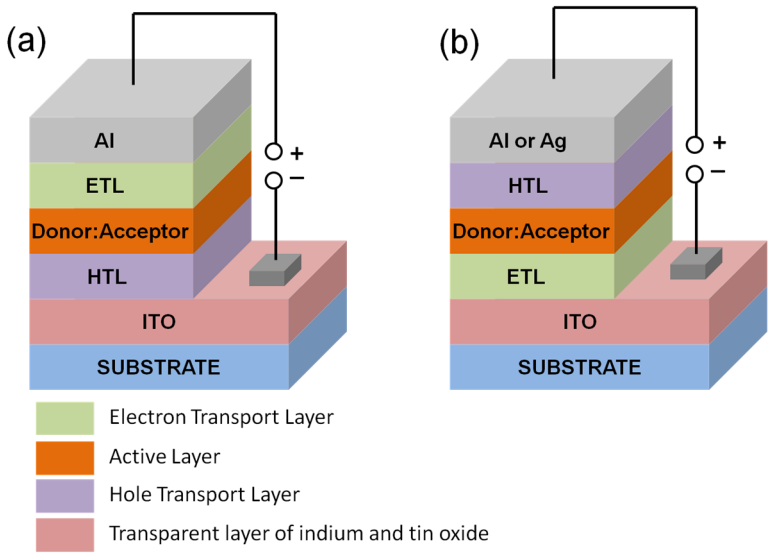

Figure 2. OPV architectures: (a) conventional (b) inverted. Adapted from [37].

The performance of OPV depends heavily on photoactive organic semiconductor materials and interface layers (HTL and ETL). It is because photon-induced charge injections in these solar cells rely heavily on the interface's physical and chemical properties, which affect the energy level

between metal contacts and organic semiconductors, obeying the so-called cascading effect formed by the energy levels of molecular orbitals [4].

BHJ cells have yet another OPV structure, the inverted architecture (Figure 2b). Inverted OPV cells (i-OPV) received special attention due to their greater stability, as they generally do not degrade for several days, even without encapsulation. Furthermore, metal oxides are the preferred materials as an interface layer in i-OPV due to the advantages of their physical and chemical properties compared to the organic interface layer [4]. Typically, these devices are composed of substrate/ITO (transparent cathode)/ZnO(ETL)/active layer/MoO_3(HTL)/Ag (anode), which have presented higher PCE and higher aging resistance [38]. This greater stability is related to a high work-function metal as a top electrode, which helps use simpler manufacturing techniques to reduce cost. In addition, the inverted structure also has more flexibility and greater photocurrent. However, the device's performance depends critically on the type of ETL material and its interface with the photoactive layer BHJ [39].

Increased stability in the inverted configuration is also related to the replacement of the PEDOT:PSS layer, such as the use of metallic nanoparticles [40] and metal oxides, such as WO_3, NiO_x, MoO_3, and V_2O_5, which have been bringing favorable electronic properties, low optical absorption at visible wavelengths and also a high level of technological compatibility [41].

The mixture of PEDOT:PSS (mass proportion: 1.00:6.11 or 1.00:6.92, depending on the provider [42] that has been widely used in conventional configuration has a high work-function (which combines with the HOMO level of commonly used donor polymers), high transparency in the visible range (greater than 80%), good electrical conductivity, and ability to reduce the surface roughness of the ITO layer. However, due to the hydrophilic nature and poor film morphology of PEDOT:PSS, low electrical properties have also been reported, while the interface between ITO and PEDOT:PSS is not stable, resulting in chemical reaction and degradation of the device. Thanks to the high acidic nature of PEDOT:PSS, ITO dissociates into the In and Sn atoms on its surface. These atoms can easily migrate to the PEDOT:PSS layer after thermal annealing, contributing to device instability [35].

As can be seen, conjugated polymers are applied to the active and secondary layers of OPV devices, as they are efficient hole-transport materials. The following will address the appropriate characteristics of its application and studies recently involved in OPV and polymer technology.

4. Polymers as donor materials

Conjugated homopolymers like polythiophenes are among the most widely used polymer structures in the manufacture of OPVs due to their good optical and electrical properties and thermal and chemical stability. Another great attraction of polythiophenes is that they allow different side chains to be added to their main structure to modify the resulting properties and increase their solubility. For example, P3HT, which has an optical Eg of 1.9 eV, achieved a good combination with fullerene derivatives ($PC_{61}BM$ or $PC_{71}BM$), becoming the reference BHJ layer in the literature [32,43,44]. Some of the p-type materials based on extensively studied homopolymers for solar cell applications are, in addition to P3HT, poly [2-methoxy-5-(2-ethyl-hexiloxy)-1,4-phenylenevinylene] (MEH-PPV) and poly(4,8-bis(5-(2-ethyloxy-hexyl)thiophen-2-yl) benzo [1,2-b:4,5-b′]dithiophene) (PBDTT) [2,45].

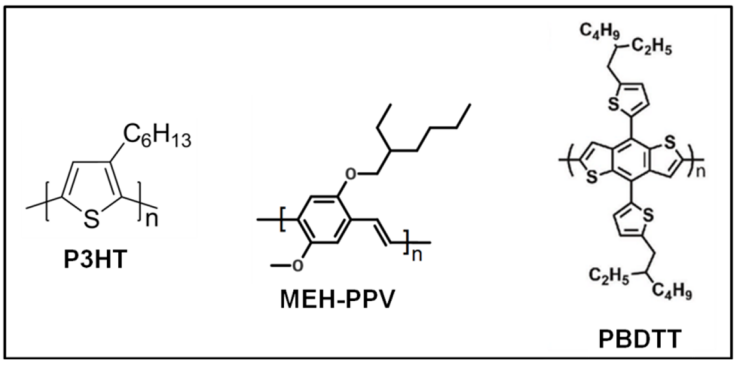

Figure 3. Chemical structures of P3HT, MEH-PPV, and PBDTT polymers.

An important approach to further develop BHJ solar cells is to incorporate a p-type conjugated polymer with a large absorption range and high molar absorption coefficient, efficient electron donor and hole transport properties, in addition to good solubility, and with tuned molecular orbital energies to meet the acceptor material demands, i.e., with a slightly higher LUMO and low HOMO concerning the acceptor. Electron acceptance (A) and electron donation (D) units in D–A copolymer (push-pull copolymer) are being studied extensively for p-polymers in OPVs. Several groups researched this direction using derivatives of the fused ring system with D character, such as fluorene, carbazole, thiophene, cyclopentadithiophene, benzodithiophene, and dithienothiophene; and with A character, like benzothiadiazole, isoindigo, quinoxaline, and benzotriazole, as units of polymeric donors [2,46,47]. Alternating polymers comprising A-D in the nucleus or main chain are among the best performing semiconductor families [45]. The push-pull polymers have D-A-D or A-D-A units in the main chain. These copolymers are very successful in modulating the physical characteristics and controlling film morphologies, leading to better device performance [2,55].

Thus, studies have been developed in donor materials engineering for the active layer, developing new materials and variations of D-A structures for application in OPVs. At this point, benzo[d][2,1,3]thiadiazole (BT), an electron-deficient heterocycle, and its halogenated derivatives have been widely used in the construction of several D-A polymers with remarkable performance.

Chen et al. (2016) [45] studied a corresponding BT isomer for copolymer synthesis. They synthesized new structures with the corresponding isomer, benzo[d][1,2,3]thiadiazole (isoBT), and their 6-fluoroisoBT (F1isoBT) and 5,6-difluoro-isoBT (F2isoBT) for the construction of alternated copolymers with tetrathiophene (P1-P3). Photovoltaic cells were manufactured in conventional architectures, ITO/PEDOT/P1-P6-$PC_{71}BM$/LiF-Al, and the performance constantly increased with the fluorination of the heterocycle, reaching values of 2.9%, 7.2%, and 9.0% for P1 (isoBT), P2 (F1isoBT), and P3 (F2isoBT), respectively.

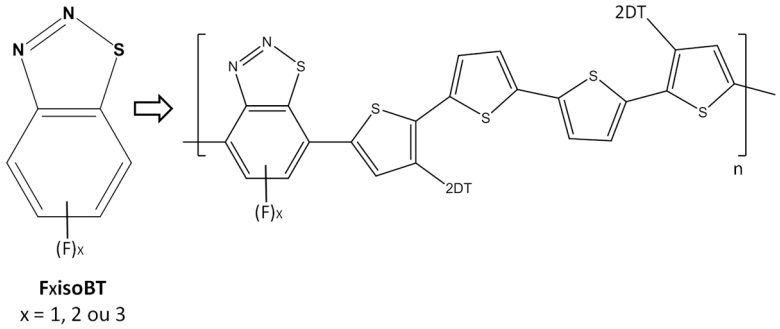

Figure 4. Chemical structures of isoBT polymers of the Chen et al. (2016) [45] study.

The electron acceptor units that are also widely used are 5,6-difluoro-2H-benzo [d][1,2,3] triazole (FBTz) and 5,6-difluorobenzo [c][1,2,5]—thiadiazole (FBT), due to its stronger electron withdrawal properties compared to their non-fluorinated counterparts. Zhong et al. (2016) [48] synthesized two wide-bandgap D-A conjugated copolymers, PDTBDT-FBTz and PDTBDT-FBT based on dithienobenzodithiophen (DTBDT) as a donor unit, with FBTz and FBT as accepting units, respectively. Both copolymers exhibited relatively wide band intervals of 1.76 eV for PDTBDT-FBT and 2.02 eV for PDTBDT-FBTz.

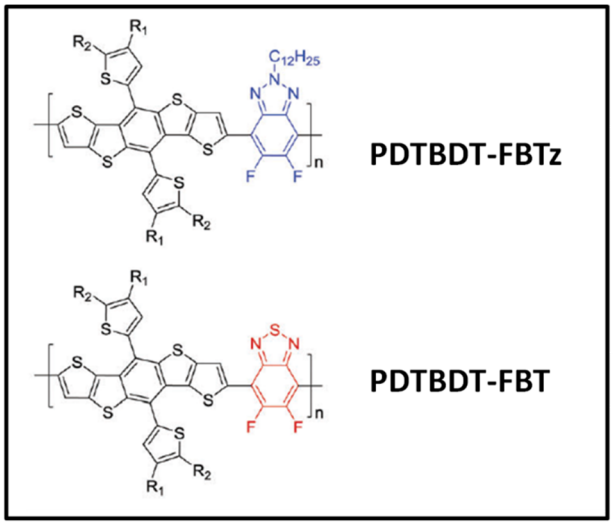

Figure 5. Chemical structures of polymers of the Zhong et al. (2016) [48] study.

Because FBT exhibits a stronger electron acceptance capability than the FBTz unit, replacing FBTz with FBT in the polymer contributed to increasing the effect of intramolecular charge transfer between D-A units, changing absorption to red, and decreasing energy levels simultaneously. The photovoltaic properties of these copolymers were investigated by manufacturing OPV devices with the ITO/PEDOT:PSS/copolymer:PCBM/Ca/Al:PCBM/Ca/Al. An additional optimization was performed by replacing $PC_{61}BM$ with $PC_{71}BM$, in which it greatly improved the performance of the device, increasing the short circuit current, reaching PCE = 5.55% (V_{OC} = 0.95 V, J_{SC} = 9.32

mA/cm^2, FF = 62.7%) for PDTBDT-FBTz and PCE = 7.45% (V_{OC} = 0.98 V, J_{SC} = 12.76 mA/cm^2, FF = 59.6%) for PDTBDT-FBT.

Halogenation of a D–A copolymer is an effective method to improve PSCs' performance further. It mainly affects the push-pull of electrons between monomer unit D and unit A [49]. Therefore, there has been great interest in introducing fluorine atoms into the polymer's conjugated structure in recent years. As approached by Chen (2018) [45], the polymers most used for the BHJ layer were those based on 3-fluorothiene, thiophene, difluorobenzotriazole (FTAZ), mono difluoro-2,1,3-benzothiadiazole (BT), and monofluorinated isoindigo, which exhibited superior performance than non-fluorinated devices. This better performance can be attributed to the reduction of donor-acceptor boundary energy levels and to the fact that it maintains the Eg of fluorinated polymers, which contributes to increasing the V_{OC} of the device. In addition, it is believed that the molecular dipole of the C-F bond, the small size of the fluorine atom, as well as its high electronegativity are highly beneficial for enhancing intermolecular interactions, improving the diffusion of the exciton, and the extraction of charges [46].

Although fluorination in conjugated polymers has many benefits, fluorination can also lead to negative effects on polymer properties, such as low solubility in an organic solvent, inadequate energy levels for excitons separation and charge transport, and large aggregation of polymers in the active layer of OPVs (Jo et al., 2015) [52]. Thus, many studies aim to understand the importance and influence of incorporating fluorine atoms into the structure of a D-A copolymer. Chen et al. (2015) [50] introduced fluoride in the meta position of the BDT unit replaced by the alcoxyphenyl group. The resulting polymer presented a lower HOMO energy level, and the polymer device:$PC_{71}BM$ exhibited a PCE of 7.02%, V_{OC} of 0.82 V, J_{SC} of 13.11 mA/cm^2, and fill factor (FF) of 65.28%. Li et al. (2016) [51] introduced two fluoride atoms into meta positions of the BDTP. They synthesized two polymers with benzodithiophene replaced with 4-alkyl-3,5-difluorophenyl as the electron donor, benzothiadiazole or benzooxadiazole as an electron-accepting unit, called PTFBDTBZS and PTFBDT-BZO, respectively. Photovoltaic devices with an active layer of PTFBDT-BZS: $PC_{71}BM$ presented PCE of 8.24% without any additive treatment. Wang et al. (2016) [38] introduced a fluorine atom into the ortho position of the BDTP unit and synthesized the polymer Po-FBDTP-C8DTBTff (P2) with the monomer 5,6-difluoro-4,7-di(4-(2-ethyl-hexyl)-2-thienyl)-2,1,3-benzothiadiazole (C8DTBTff), comparing with the reference polymer PBDTP-DTBTff (P1), without F in the phenyl group. Thus, they observed that the insertion of F atom in the ortho position of the BDT unit replaced by alkoxyphenyl greatly decreased the HOMO energy level of P2, increasing the V_{OC} to 0.94 V. Meanwhile, the incorporation of fluorine atoms in the conjugated side chain of the polymer also increased the charge mobility and contributed to the improved morphology of the active layer. These synergistic effects increased the PCE of P2-based devices to 8.10% after the additive treatment.

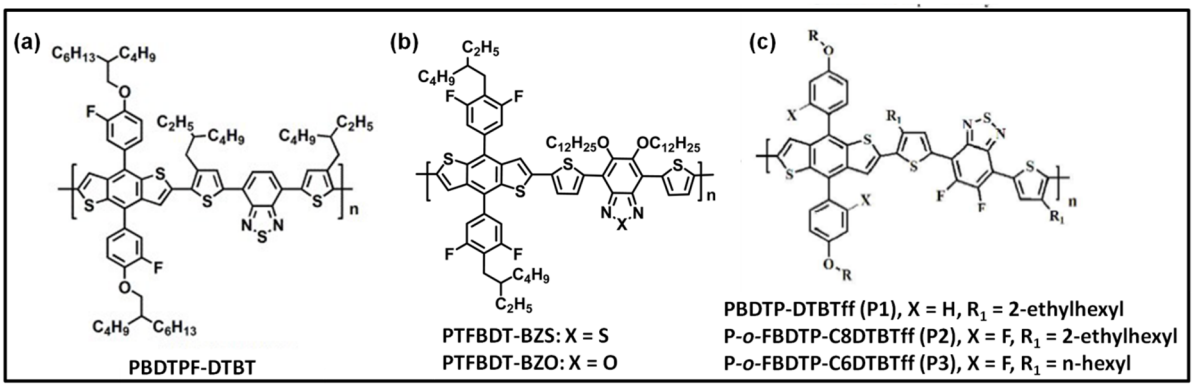

Figure 6. Chemical structures of polymers of the (a) Chen et al. (2015) [50], (b) Li et al. (2016) [51] and (c) Wang et al. (2016) [38].

Jo et al. (2015) [52] investigated the effect of fluorination on polymers' photophysical properties and the performance of OPVs devices. Thus, three fluorinated D-A polymers with different fluorination numbers were synthesized, consisting of 3,30-difluoro-2,20-bithiophene (unit D) and BT (unit A) with and without fluorination; the total number of fluorine atoms in the polymers was controlled by the number of fluoride replacement in the BT unit. It was observed that the additional fluoride substitution in the BT unit further decreases the energy levels of the frontier and improves the molecular order of conjugated polymers, even when there are already two fluoride atoms in unit D. When compared with the polymer with non-fluorinated BT, the polymer with mono-fluorinated BT showed higher performances, with higher PCE of 9.14%, while the polymer with difluorinated BT exhibited a lower performance, with PCE of 6.43%, which was justified by the higher recombination rate and lower hole mobility.

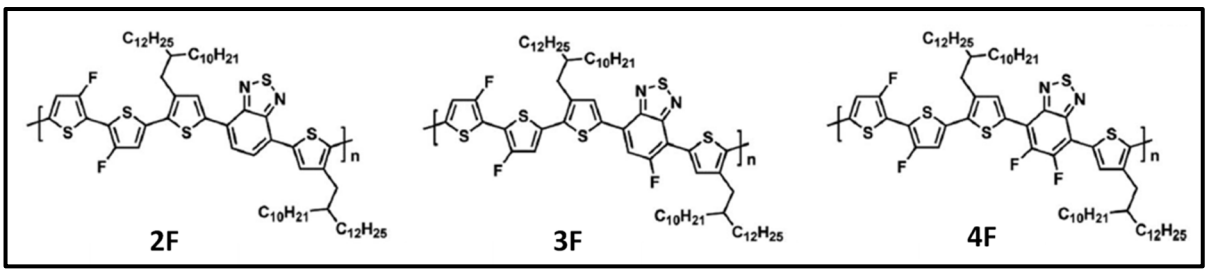

Figure 7. Chemical structures of polymers of the Jo et al. (2015) [52].

Chlorination of polymer donors is also an effective strategy to increase V_{OC}. Introducing a chlorine atom with strong electronegativity and accommodating delocalized electrons can efficiently deepen the HOMO and LUMO levels. In D-A copolymers, a π-bridge between D and A units is sometimes needed to reduce the steric hindrance and improve the molecular planarity. In some cases, a conjugated side chain is added to enhance the coplanarity of the main chain, consequently expanding the absorption band to longer wavelengths [53].

Another approach that has been used is the development of polymers with π (p) between D-A units, the so-called D-p-A copolymers. The p-conjugated bridges crucially influence the electronic

structure of the main polymer chain and the interaction between units D and A; therefore, they notably affect the stereostructure and, consequently, the photophysical, electrochemical, charge-carrying, and photovoltaic properties of these copolymers [54,55]. Yan and coworkers (2018) [56] studied the influence of π bridges' insertion between alternating units in D-A copolymers. The new alkoxy-BDT-alt-FBTA-based copolymer with TT bridges, called J41, showed a deeper HOMO energy level of −5.39 eV and a slightly offset absorption to blue compared to J40, probably caused by some main chain torsions due to larger thienothiophene units [3,2-b]. OPVs with J41 as a donor and ITIC, a non-fullerene acceptor (NFA) substitution PCBM, demonstrated a PCE of 8.74% with a higher V_{OC} of 0.93 V, which is significantly improved compared to the 6.48% PCE with V_{OC} 0.89 V for the corresponding OPVs with J40 as a donor.

Bin et al. (2014) [57] synthesized several new D-p-A copolymers with benzodithiophene ((BDT)) or dithienosilol (DTS)) as a donor unit, alkylthiophene (TA) or thieno[3,2-b] thiophene (TT) as a bridge (p), and benzodithiophene-4,8-dione (BDD) as an accepting unit, generating the copolymers PBDT-AT, PDTS-AT, PBDT-TT, and PDTS-TT. For the four polymers, the difference in position and shape of the absorptions was mainly due to the different structures of the p-bridges and donors. Compared with PDTS-AT, the absorption spectrum of PBDT-AT is wider and with remarkable displacement to red (568 *vs*. 534 nm), which indicated different electron donation forces of these donor units (BDT *vs*. DTS). A similar phenomenon can be found to compare PBDT-TT with PDTS-TT. Also, the PDTS-TT exhibits a red deviation from the PDTS-AT, revealing the effect of the different p-bridges on the optical properties of the D-p-A copolymers. In addition to the electrochemical properties, the different p-bridges resulted in a considerable difference in HOMO energy levels for PBDT-AT and PDTS-AT compared to PBDT-TT and PDTS-TT. Concerning photovoltaic properties, the devices were mounted in a conventional configuration of ITO/PEDOT:PSS/polymer:$PC_{70}BM$/Ca/Al, and it was observed that with the optimization of proportion and concentration of additive diiodoctane (DIO), the OPVs based on PBDT-AT presented a PCE of 5.46% with DIO at 5% in v., and with treatment with methanol reached 5.91%, which is greatly improved compared to the corresponding polymer without the p-A bridge. For the other polymers based on PDTS-AT, PBDT-TT, and PDTS-TT, their best performance after optimization was 3.06%, 1.45%, and 2.45%, respectively.

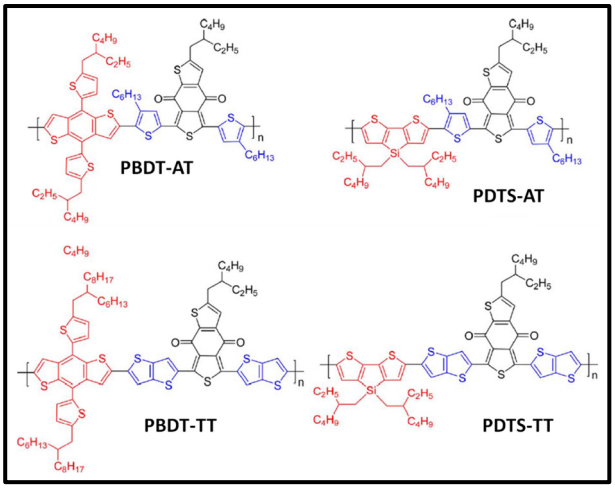

Figure 8. Chemical structures of polymers of the Bin et al. (2014) [57]. Adapted from [57].

The development of terpolymers has also been studied to expand the absorption spectrum and even achieve some synergistic effects. For example, Akkuratov et al. (2017) [58] conducted a systematic study of a family of statistical fluorene-carbazole-TTBTBTT (T-thiophene, B-benzothiadiazole) terpolymers, with a variable proportion of fluorine for carbazole (X:Y). The polymers P1 (0:100), P2 (100:0), and the P3 a-f series (with variation in molar concentration from 5:95 to 90:10) were obtained. This study showed that the maximum of the main absorption bands in the spectra of the P1 and P2 regioregular copolymers were close to each other at 605 and 609 nm, respectively. In contrast, only 10% of carbazole units in P3f changed the maximum absorption to 624 nm compared to the pure P2 fluorine-based copolymer. Simultaneously, the introduction of 5% of fluorine units (P3a) could take off the maximum absorption band further to 643 nm, compared to the pure P1 carbazole-based copolymer. Also, increasing the fluorine content in polymers by up to 70–90% (P3e-f) resulted in a noticeable anodic change in oxidation waves. These results imply that only a small concentration of carbazole units (10% in P3f) significantly reduces the material's oxidation potential. Thus, the study shows that the change in polymers' molecular composition significantly affects their characteristics, such as absorption spectrum, extinction coefficients, boundary position, energy levels, and charge carrier mobility. Energy conversion efficiencies of 6.4 to 7.0% were obtained for the best performing carbazole-rich and fluorene-rich terpolymers. At the same time, optimizing the morphology of the mixture can lead to better photovoltaic performance up to theoretically possible values of 9 to 11%.

In addition to all the engineering involved in developing the donor polymer, there must be an ideal combination with the active layer's activator. Other acceptors, different from fullerene derivatives, with push-pull copolymer units, have been widespread in recent years. For example, D-A copolymers based on the skeleton of benzodithiophene-alt-benzotriazole (BTA) as donor materials are highly efficient for OPV devices without fullerene. Several organic acceptors, such as thiophene-fused benzotriazole (BTAZT) and thiophene-fused benzothiadiazole (BTT), to build D-A copolymers for OPVs have been reported, in which it was found that the fusion of a thiophene ring next to the BTAZ or BT unit can stabilize the quinoid population of the polymer structure (backbone) of the D-A conjugation, to strengthen the effect of intramolecular charge transfer and promote the increase of J_{SC} [59,60].

Jiang (2018) [61] developed a new organic acetazol based on fluorinated BTA, the thieno[2′,3′:4.5]benzo[1,2-d][1,2,3]triazole (fBTAZT), in which fluor (F) was introduced into the α position of the thiophene ring in the BTAZT unit. Thus, two D-A copolymers were synthesized based on the fBTAZT unit with fluorinated BDT and BDT units, respectively, called PfBTAZT-BDT and PfBTAZTfBDT. Fluorination in the BTAZT and BDT units was found to have a synergistic effect on HOMO-LUMO energy levels and the photovoltaic performance of the corresponding D-A copolymers. In fact, the polymer PfBTAZT-fBDT with fluorine atoms in the BTAZT and BDT blocks shows the deepest HOMO level, and the corresponding solar cell device exhibits a relatively high V_{OC} of 0.77 V and PCE of 6.59%, compared to the 6.04% PCE obtained by the PfBTAZT-BDT copolymer.

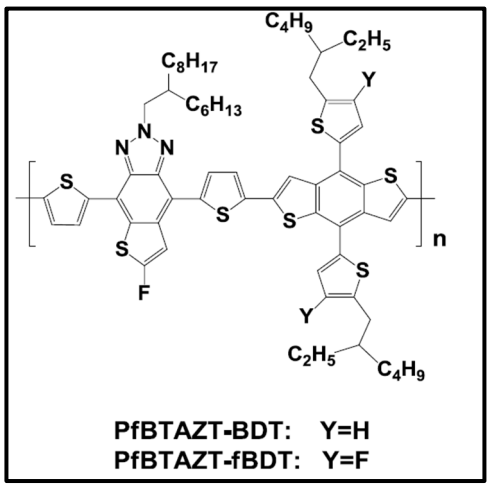

Figure 9. Chemical structures of polymers of Jiang et al. (2018) [61].

Chang et al. (2018) [62] developed a new PBFTT narrowband copolymer, based on 4,8-bis(5-(2-ethylhexyl)-4-fluorothiophen-2-yl)benzo[1,2-b:4.5-b']dithiophene (BDT-2F) as a donor unit and octyl-3-fluorothieno[3,4-b]thiophene-2-carboxylate (TT) as an accepting unit. This copolymer was used as donor material for OPV without fullerene (NFA). Compared to the analog polymer PTB7-Th, PBFTT exhibits a similar absorption spectrum with a slight deviation to blue while exhibiting a deeper HOMO energy level of −5.47 eV and slightly higher hole mobility. The OPV device based on PBFTT:ITIC presented a PCE greater than 9.1% with a V_{OC} of 0.94 V, a J_{SC} of 16.0 mA/cm^2, and a fill factor (FF) of 60.5% compared to the 6.8% PCE for PTB7-Th-based devices:ITIC (V_{OC} of 0.81 V, J_{SC} of 14.2 mA/cm^2 and FF of 59.1%).

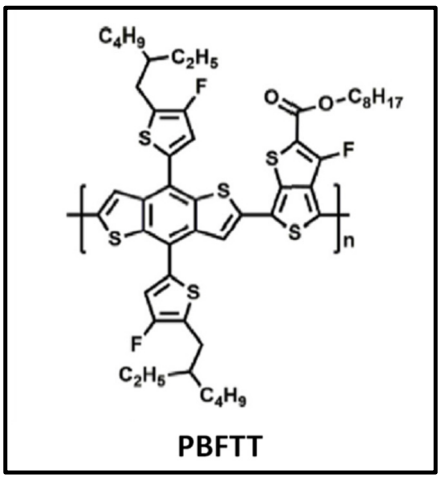

Figure 10. Chemical structures of polymers of the Chang et al. (2018) [62].

Energy conversions greater than 16% have been reported in advanced organic solar cells. Sun et al. (2018) [63] designed and synthesized a poly[(thiophen)-alt-(6,7-difluoro-2-(2-hexyldecyloxi) quinoxaline)] (PTQ10), based on the concept of donor-acceptor copolymer (D-A), using a simple thiophene ring as a donor unit and quinoxaline replaced by difluorine as an acceptor unit. The

alcoholic side chain has been added to the quinoxaline unit to ensure good solubility and improve polymer absorption, while difluorine substituents are designed to reduce the HOMO energy level and increase donor polymer hole mobility. OPV device with PTQ10-optimized as a donor and IDIC as an acceptor demonstrates an impressive PCE of 12.70%. In addition, the devices showed good reproducibility and high tolerance to the thickness of the active layer with a PCE above 10%, even at an active layer thickness of 310 nm.

Fan and collaborators (2019) [64] developed fullerene-free devices with the electron donor polymer P2F-EHp, which consists of a weak benzo-based electron donor unit [1,2-b:4,5-b′] dithiophene (BDT) and a weak pyrrole-based electron withdrawal unit [3,4-f]benzotriazole-5,7(2H, 6H)-dione (TzBI); and two non-fullerene acceptors, BTPT-4F and BTPTT-4F (also called Y6). The composites P2F-EHp:BTPT-4F and P2F-EHp:BTPTT-4F showed complementary absorption and corresponding energy levels, favorable to collecting solar photons. The absorption of P2F-EHp:BTPTT-4F ranged from 400 to 900 nm, covering a wide range of visible-NIR solar radiation, while the P2F-EHp:BTPT-4F mixture exhibited a narrower absorption profile below 800 nm. The devices manufactured were of conventional configuration, with ITO/PEDOT:PSS/active layer (120 nm) with D:A of 1:1.2/PFNDI-Br/Ag. In addition, a thin layer of the cathodic interface PFNDI-Br was used to facilitate electron extraction. Dibenzyl ether (DBE) was used as a solvent additive for the morphology adjustment. By adjusting the photoactive layer's morphology, the P2F-EHp:BTPTT-4F based device has achieved an unprecedented PCE of more than 16%, suggesting the great promise of materials corresponding to high-performance organic solar cells.

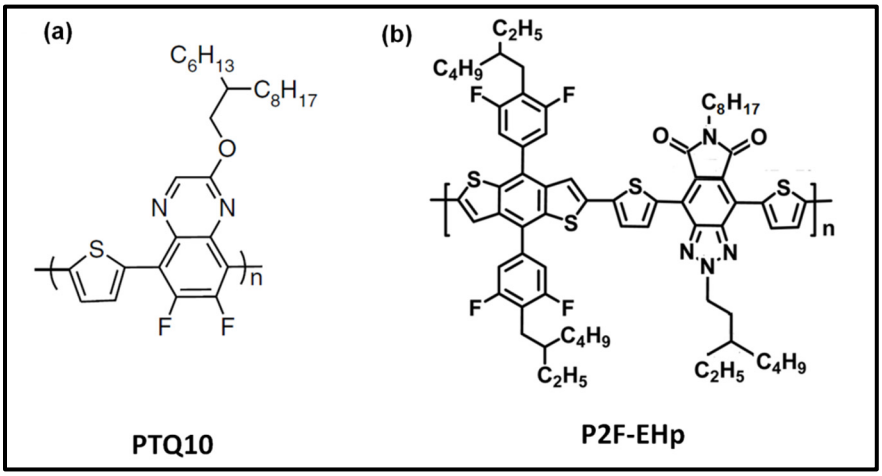

Figure 11. Chemical structures of polymers of the (a) Sun et al. (2018) [63] and (b) Fan et al. (2019) [64].

Xiong et al. (2019) [65] synthesized a D16 copolymer based on a molten ring thiolactone unit, 5H-dithieno[3,2-b:2',3'-d]thiopiran-5-one (DTTP), with Y6 non-fullerene acceptor. Conventional solar cells with an ITO/PEDOT:PSS/active layer/PDIN/Al structure were assembled to evaluate the donor polymers' performance. The D/A ratio, the thickness of the active layer, and the additive were optimized. The best performance was D16:Y6, with a PCE of 16.22%. To improve D16 solar cells' efficiency further, devices were manufactured using the Ag electrode, considering that Ag has greater reflectance in the visible and near-infrared regions. The D16 cell with Ag electrode shows improved

external quantum efficiency (EQE) and superior J_{SC} compared to Al electrode cells. The best cell presented a PCE of 16.72%, with a V_{OC} of 0.85 V, a J_{SC} of 26.61 mA/cm^2, and an FF of 73.8%.

Liu et al. (2020) [66] synthesized a more efficient D18 copolymer donor using a molten ring acceptor unit, dithieno[3',2':3,4;2",3":5,6]benzo[1, 2-c][1,2,5] thiadiazole (DTBT). Compared to DTTP (base for copolymer D16), DTBT has a larger molecular plane and offers D18 greater hole mobility. Solar cells with an ITO/PEDOT:PSS/D18:Y6/PDIN/Ag structure were made to evaluate the performance of D18. The D/A ratio, active layer thickness, additive content, and solvent vapor annealing time (SVA) were optimized. The best D18:Y6 cells presented a PCE of 18.22%, with a V_{OC} of 0.859 V, a J_{SC} of 27.70 mA/cm^2, and an FF of 76.6%. These cells have a D/A ratio of 1:1.6 (by mass), an active layer thickness of 103 nm, no additive, and a chloroform SVA for 5 minutes. D18:Y6 solar cells resulted in a PCE of 18.22% (certified 17.6%).

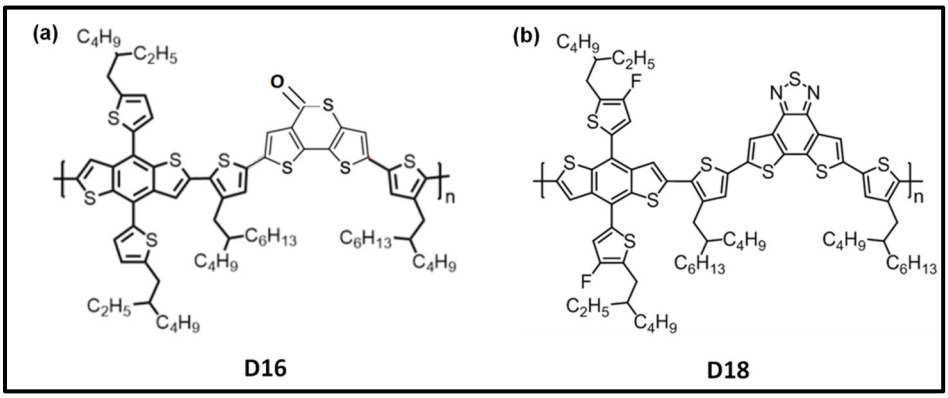

Figure 12. Chemical structures of polymers of the (a) Xiong et al. (2019) [65] and (b) Liu et al. (2020) [66].

Since the developed polymer presents promising characteristics for OPV technology, a compatible architecture and an efficient combination with the acceptor material are required to achieve significant device efficiencies. This way, it will be briefly addressed about the different acceptors being used in the active layer in the following section.

5. Active layer acceptors

The active layer of OPVs is composed of a conjugated polymer as a p-type semiconductor, an electron donor, which mixes with a fullerene derivative or an organic n-type semiconductor, non-fullerenes, as an acceptor. Efficiency, stability, and cost are the three most crucial issues that should be taken into account for the commercial application of these units, and donor photovoltaic materials and acceptors play an essential role in increasing the PCE, improving the ability, and reducing the cost of organic solar cells [63].

Almost exclusively studied acceptors were the soluble fullerene methyl ester of the butyric acid derivatives ($PC_{61}BM$ or $PC_{71}BM$), mainly due to its excellent n-type semiconductor characteristics favorable compatibility with butyric acid derivatives a large number of donor materials [10].

These fullerene derivatives, $PC_{61}BM$ and $PC_{71}BM$, allowed reports of remarkable efficiencies. Although $PC_{71}BM$ generally produces larger photocurrents, thanks to improved absorption in the

visible compared to $PC_{61}BM$ and more favorable interpenetration properties, both have the same LUMO values that considerably limit the V_{OC} of the devices [32].

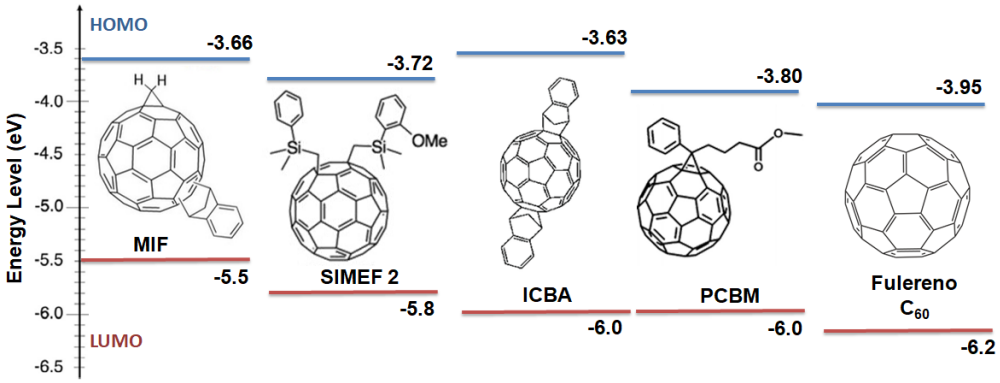

Figure 13. Energy level of HOMO and LUMO orbitals of fullerene derivatives.

In addition to all the engineering involved in searching for an efficient active layer, some projects seek to improve the fullerene-derived receptors. Matsuo et al. (2012) [67] used dimethyl (o-anisyl)silylmethyl)(dimethyl phenylsilylmethyl), C_{60}-fullerene (SIMEF2), which is a promising fullerene-based electron acceptor with high levels of LUMO and with the possibility of reaching a high J_{SC} due to its high electron mobility. This study employed a SIMEF derivative in inverted photovoltaic devices based on P3HT. The devices that use SIMEF exhibited a higher V_{OC} than those that used a standard electronic acceptor material, namely the $PC_{61}BM$. Also, no reduction in J_{SC} was observed, demonstrating a new possibility to improve i-OPV devices in future research.

Another fullerene derivative, indeno-C_{60} bisadduct (ICBA), was also a good alternative acceptor. The ICBA has a higher LUMO level than the PCBM, resulting in a higher V_{OC}. Thus, P3HT-based devices with ICBA as acceptor resulted in cells with V_{OC} values of 0.84 V and improved PCE of 6.5% [68].

Efforts to modify the fullerene structures to improve the device's performance have not been successful due to flexibility in molecular design, difficult purification, lack of morphological stability, and limited light absorption in the visible region [10]. Furthermore, despite the initial success, the intrinsic capacity of light capture of fullerenes was weak, limiting the application and efficiency of the devices [66]. Thus, studies of OPV without fullerene have been increasingly explored.

Organic semiconductors NFA (non-fullerene acceptor) replace fullerene-based materials as electron receptors, mainly because the active fullerene-free layers present lower energetic losses [3]. NFAs can be small molecule derivatives (SM) or polymer derivatives. Strategies of NFA structures are using "twisted" molecules and bulky "out of plane" side chains, once 3D structures prevent aggregation and excessive crystallinity, increasing the solubility.

In addition, these new acceptors have strong and easily adjustable absorption characteristics compared to fullerene-type structures. Therefore, they enable the levels of molecular frontier orbitals to be precisely controlled by the systematic modification of molecular structures, which results in a higher current and voltage in non-fullerene solar cell devices [10].

The great difficulty of these acceptors is that they have an even greater dependence on donor materials. Therefore, in an attempt to identify donor materials for OPVs without fullerene, some criteria should be considered:

i) Donor energy levels must be appropriate for a high-performance non-fullerene acceptor to obtain exciton dissociation driving force, small energy loss, and high V_{OC} [30].
(ii) The donor shall have complementary absorption with the non-fullerene acceptor. The electron donor polymers are always designed as broadband species (WBG) to match the narrowband non-fullerene acceptors (NBG) and thus achieve high J_{SC} [69].
iii) The donor must have morphological compatibility with the acceptor to achieve the optimal phase separation, extraction and good charge transport, high FF, and high J_{SC} [11,30].

A series of NFAs was correlated with their respective energy levels, as shown in Figure 14.

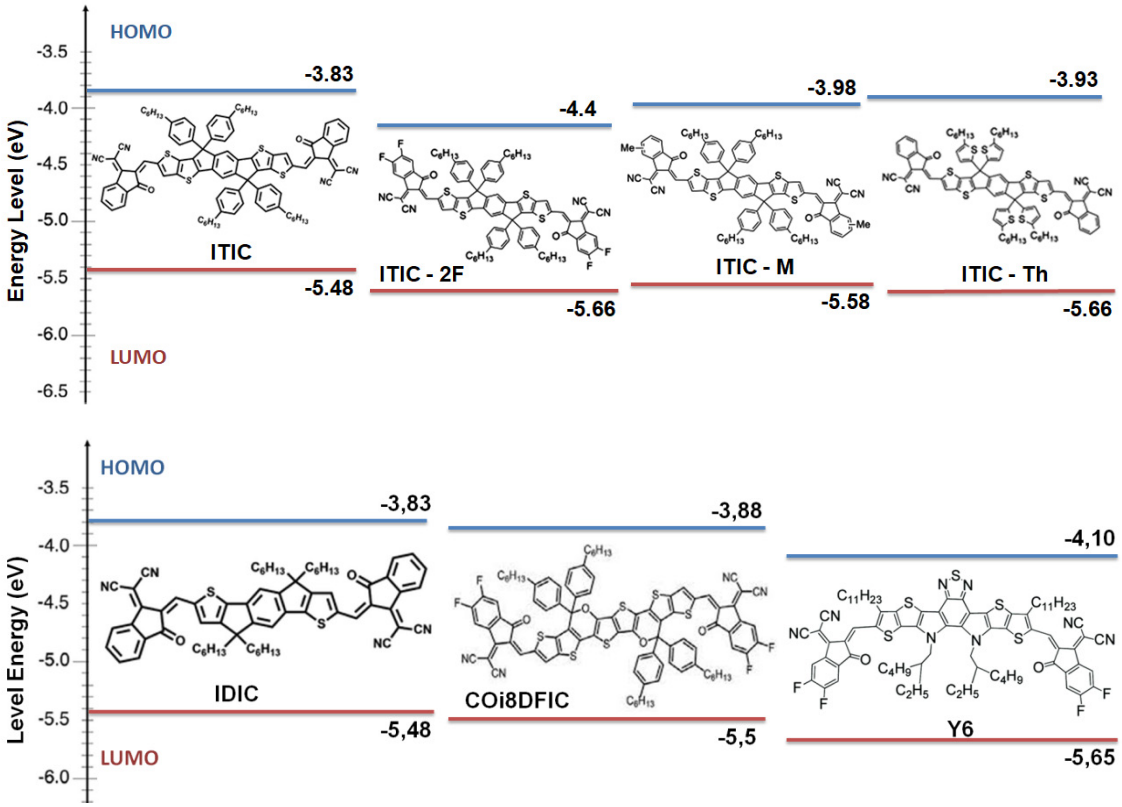

Figure 14. Energy level two orbitals HOMO and LUMO of two different fullerenes acceptors.

Low-bandgap NFAs such as ITIC and IDIC attracted much attention due to the advantages of strong and wide absorption, easy-to-tune electronic energy levels, and high morphological stability compared to fullerene derivatives [63]. Also, they have a strong light capture capacity in the frequency range from near-infrared (NIR) to visible and good electron mobility, and they provide higher J_{SC} and higher PCE in solar cells [65].

Li et al. (2018) [70] performed a comparative study between IT-M and IT-4F acceptors with a PBDB-TF copolymer. They observed that the push-pull effect improves the dipole moment in IT-4F over IT-M, improving the miscibility of IT-4F when mixed with the polymer. It results in higher purity domains in the PBDB-TF:IT-4F combination contributing to better PV performance. In addition, this effect also contributes to a reduction in vibrational relaxation, reducing energy losses in the final device, which achieved an energy conversion efficiency of 13.7% in devices based on PBDB-TF:IT-4F.

Polymeric NFAs, until today have shown lower performance than SM so far, although they have

great advantages in practical OPV applications. Due to stable polymer/polymer blend film morphology, they form active layers with improved robustness. Moreover, they have higher printing processability and better performance for flexible applications due to the improved mechanical properties of polymers. Polymers best suited for NFAs have narrow bandgaps, strong light absorption in the 500–800 nm region, efficiency for molecular packaging, good charge transport, and miscibility/compatibility with various donor materials.

NFAs must have high crystallinity. Acceptor-donor-acceptor (ADA) copolymer with fused ring acceptor, efficient π-π stacking, facilitating the transport of electrons; with out-of-plane substituents (increase solubility) are very suitable. Moreover, inserting electron-rich heteroatoms, O or N, increases the central unit's electron-donating capacity is another strategy to improve the light-harvesting capacity. ADA copolymers with bridges between the A-terminal and D-core units are being used. Linear or branched side chains are also grafted at different positions on the D, affecting solubility and miscibility, influencing optoelectronic and molecular packing properties.

It is important to mention that NFAs facilitate exciton dissociation and exhibit longer exciton diffusion length and lifespan. In addition, they can have large domain sizes: 20–50 nm, reducing energy loss (exciton extinction) and increasing light absorption.

6. Active layers of ternary organic solar cells

In addition to the development of new active materials, innovation in the device optimization process, and interfacial engineering, ternary strategies have emerged as an improvement in the performance of solar cells [71]. Introducing the third component in bulk heterojunction organic solar cells has become an effective strategy to improve photovoltaic performance [71]. Ternary OSCs generally consist of three components in the photoactive layer: a dominant donor:acceptor (D:A) system, as in simple OSCs, and a third component, which can be a donor (D) or an acceptor (A) [73].

A successful ternary system formed by two donor materials paired with one acceptor (2D/1A) or one donor paired with two acceptors (1D/2A) can contribute to increased device performance. A good interaction of the dominant active layer with the third component can facilitate energy and charge transfer and improve the molecular ordering within the photoactive layer. These factors enhance the generation and transport of charges [73]. Furthermore, these systems often feature complementary absorption, reduced voltage loss, minimal charge recombination, which allows for improved OSC ternary short circuit current (JSC) and fill factor (FF) [71,72].

But for that, the choice of the third component is very important. Although the active layer of BHJ has more D/A interfaces, controlling the vertical phase separation gradient is difficult, and there may be isolated islands in its interior, which means that electrons and holes are not effectively dissociated and forwarded to the electrodes. In this way, the third component can act as a recombination center and lead to an unfavorable morphology, seriously compromising the charge generation and transport process [73,74].

At first, the success of the ternary strategy focused mainly on combining two polymeric donor materials and a fullerene derivative [75]. However, recent works have achieved high PCE with polymeric and small-molecule donor material and non-fullerene acceptors.

Kumari and collaborators (2018) [76] studied the solubility properties in a series of non-halogenated solvents, of a ternary mixture with two donors, poly(4,8-bis(5-(2-ethylhexyl)thiophen-2-yl)benzo[1,2-b;4,5-b']dithiophene-2,6-diyl-alt-(4-(2-ethyl

hexyl)-3-fluorothieno[3,4-b]thiophene-)-2-carboxylate-2-6-diyl (PTB7-Th) and small molecule of benzo[1,2-b;4,5-b']dithiophene (DR3TSBDT)), and an acceptor ([6,6]-phenyl-C_{71}-butyric acid methyl ester, $PC_{71}BM$), achieving an energy conversion efficiency of 12.3% (certified 11.94%) in the developed non-halogenated processing system.

Xie et al. (2020) [77] synthesized PBDT-TPD, a wide-bandgap donor conjugated polymer. The low crystallinity PBDT-TPD polymer and the ITIC-4F acceptor were used to manufacture the binary OSCs, while the ternaries relied on introducing a small molecule, high crystallinity acceptor C8IDTT-4Cl. A ternary device based on the mixture PBDT-TPD:ITIC-4F:C8IDTT-4Cl showed a better PCE of 9.51% with a simultaneous improvement of the short circuit current density to 18.76 mA/cm^2 and the fill factor up to 67.53%. Values higher than those of binary devices based on PBDT-TPD:ITIC-4F (PCE 8.70%) and PBDT-TPD:C8IDTT-4Cl (PCE 7.55%).

Sharma (2020) [73] developed ternary organic solar cells (OSCs) that employ the conjugated polymer PTB7-Th and the small molecule p-DTS(FBTTh$_2$)$_2$ as donors and the non-fullerene molecule IEICO-4F as the acceptor, achieving a conversion efficiency of 10.9% energy for PTB7-Th: p-DTS(FBTTh$_2$)$_2$:IEICO-4F with 15% by weight of p-DTS(FBTTh$_2$)$_2$, compared to 9.8% PCE for PTB7-Th: IEICO-4F CSOs. Furthermore, the authors confirm that the addition of the small-molecule donor in the PTB7-Th:IEICO-4F binary mixture improved the molecular ordering and crystallinity of PTB7-Th due to the favorable interaction that provided 3D textured structures. This improved molecular ordering contributed to increased exciton generation rate, exciton dissociation, charge collection, and reduced charge recombination.

Chen et al. (2020) [71] developed a new non-fullerene acceptor based on the central fused core of benzo[1,2-b:4,5-b'] dithiophene (BDT) with asymmetric alkoxy and thienyl side chains, TOBDT. The alkoxy unit helps narrow the bandgap, and the thienyl side-chain helps to improve the intermolecular interaction. As a result, TOBDT showed a low optical bandgap of 1.41 eV with energy levels suitable to pair with the PM6 wide-bandgap donor, which has a deep HOMO energy level. The solar cell with the PM6:TOBDT binary mixture achieved a PCE of 11.3% with a Jsc of 18.7 mA/cm^2, a V_{OC} of 0.89 V, and a fill factor (FF) of 0.68. In the ternary device, an additional highly crystalline acceptor, IDIC, was added to provide complementary absorption in the device. The addition of IDIC helped to reduce the photovoltage loss and balance the charge transport properties, which contributed to improved Jsc, V_{OC}, and FF values simultaneously, leading to a 14.0% PCE for the ternary device.

Xiao and collaborators (2021) [72] fabricated a series of fullerene-free ternary solar cells based on a wide-bandgap acceptor, IDTT-M, a narrow bandgap acceptor, Y6, and the wide-bandgap donor polymer PM6. Morphological and electronic characterizations reveal that IDTT-M was incorporated into the Y6 domains without disrupting their molecular packaging and sacrificing their electron mobility, working synergistically with Y6 to regulate the PM6 packaging pattern, increasing hole mobility and reducing recombination. Compared to their binary counterparts, the optimized ternary solar cells (PM6:Y6:IDTT-M = 1:1.02:0.18) provided the best PCE of up to 16.63% with simultaneously enhanced JSC from 25.41 to 25.81 mA/cm^2, V_{OC} from 0.841 to 0.872 V, and FF from 72.45% to 73.89%.

7. Other layers of organic solar cell

Just as the photoactive layer is essential to the device, interfacial layers also play an important role in obtaining a high FF. To improve photovoltaic performance, the control of morphology and the layers' design become two main topics for OPV [20,78]. Some criteria must be followed to obtain optimal interfacial layers, such as: (i) adequate energy levels to align the materials in the BHJ to reduce the contact energy barrier; (ii) interactions to ensure sufficient internal tension; (iii) good solubility or dispersion to ensure the formation of the film; (iv) adequate wettability in the lower layers to avoid defects during film formation; (v) wettability suitable for processing with solvents, thus simplifying manufacturing procedures [19,20].

One of the approaches is enhancing the device using a double layer of HTL. Singh et al. (2016) [79] reported improved PCE using double HTL in BHJ cells due to the greater mobility of charge carriers. In turn, Kageyama et al. (2011) [80] reported that MoO_3 between the LiF and Al electrode resulted in greater ease of exciton formation and its dissociation in charge carriers.

Xu et al. (2018) [78] developed a highly transparent and thickness-insensitive hybrid ETL, processable in solution, with enhanced extraction and electron transport properties for high-performance polymer solar cells. Through the incorporation of Cs_2CO_3 in the poly[(9,9-bis (6′-((N, N-diethyl)-N-ethylammonium))-hexyl)-2,7-fluorene)-alt-1,4-diphenylsulfide]dibromide (PF6NPSBr) and application as ETL, the PCE of the resulting polymeric solar cells was significantly improved due to good interfacial contact, alignment of energy level and, therefore, easy electron transport in the OPV device. With the conventional structure of the device employing poly{4,8-bis[5-(2-ethyl-hexyl)thiophen-2-yl]benzo[1,2-b:4,5-b′]dithiophene-2,6-diyl-alt-3-fluoro-2-[(2-ethyl-hexyl)carbonyl]thieno[3,4-b]thiophene-4,6-diyl} (PTB7-Th) as donor and $PC_{71}BM$ as acceptor, devices with hybrid ETL with PCE of 8.30 to 9.45% within a wide range of ETL thickness. A remarkable PCE of 10.78% was achieved with the thick active layer of poly(2,5-thiophene-alt-5.5′-(5,10-bis(4-(2-octyldodecyl)-thiophen-2-yl)naphto[1,2-c:5,6-c′]bis([1,2,5]thiadiazole)) (PTNT812):$PC_{71}BM$.

Sachdeva et al. (2018) [81] studied a double layer of HTL on OPVs. Three devices were manufactured consisting of FTO-coated glass substrate, MoO_3 (anodic contact), TAPC, (4,4′-cyclohexylidenebis[N, N-bis (4-methylphenyl) benzenamine]), and C_{70}. Concerning HTL, the first device was produced without HTL. In the second, the HTL consists of LiF, and the third with LiF and MoO_3. The electrode comprises Al. This study revealed improvements in the performance of the OPV device with the insertion of HTL. The J_{SC} of the device with LiF decreased to 4.91 mA/cm^2 (the measurement was 5.81 mA/cm^2 from the reference cell without HTL). The PCE of the device with LiF was measured at 2.47%, while the reference cell's efficiency was 1.89%. However, a decrease in the LiF device's EQE (External Quantum Efficiency) was observed. With the double layer of HTL (LiF/MoO_3), the J_{SC} of the device increased to 6.18 mA/cm^2 and obtained PCE of 3.51%, demonstrating that the double layer's insertion improved the PCE of the OPV device.

Another evolution reported in the literature is using ZnO on ITO electrodes as an ETL layer in organic solar cells. Some studies can be found on the effects of the amount of Al dopant, surface roughness, and nanostructure with gradient distribution of the dopant Al in ZnO (gradient Al-doped ZnO, AZO) on the efficiency of OPVs [82]. However, thermal expansion inevitably occurs in the substrate with ITO during the AZO annealing process, affecting the crystal qualities and optical properties of AZO thin films, increasing the density of defects in the film surfaces. This film quality

can be improved by introducing a damper layer and doping. On the other hand, Yu et al. (2015) [82] used a multi-damping layer of ZnO doped with Al gradient distribution for the first time, used in the ETL of cells with inverted configuration. Its effect on the photovoltaic performance of inverted OPVs was systematically studied and compared with devices containing a ZnO layer. ETL presented smoother surfaces, more efficient light transmission, better film qualities, and higher conductivities, contributing to the device's increased photovoltaic performance. The PCE of this device was 62.5% higher than that of the device with an ETL layer containing only ZnO. Salem and collaborators (2017) [39] demonstrated that ZnO nanoparticles produced by the sol-gel process and with annealing treatment could be used as an ETL in inverted BHJ polymer solar cells, as well as employing CuI as an HTL compared to the use of conventional HTL constituted of PEDOT:PSS. Three different devices were manufactured: Device A: ITO/ZnO/MEH-PPV nanoparticles:$PC_{61}BM$/PEDOT:PSS/Ag, Device B: ITO/ZnO/ZnO nanoparticles macrospheres/MEH-PPV: $PC_{61}BM$/PEDOT:PSS/Ag, and Device C: ITO/ZnO/MEH-PPV nanoparticles:$PC_{61}BM$/CuI/Ag. The effect of another layer of mesoporous ZnO microspheres connected to ZnO nanoparticles has also been investigated. The highest PCE value of 1.35% was reached for device C, which is 275% higher than the value obtained when CuI was replaced by PEDOT:PSS. Analyses of structural and optical characteristics indicated that using ZnO nanoparticles alone as ETL, together with CuI as HTL, could reduce trap-assisted recombination and charge accumulation at its interface, beneficial for improved device performance.

Transparent conductive oxide thin films have been extensively studied as key components in numerous optoelectronic materials. However, in traditional OPVs, PEDOT:PSS is used, a certain limitation is generated in the device due to its chemical instability. Then, to find effective HTL, Pandley and collaborators (2018) [83] performed the deposition of an ultrafine metallic layer of iridium as an interface between the ITO and the active layer of the OPV cell. Ultrafine iridium was deposited as a surface modifier (USM) in ITO-coated glass substrate with active layers P3HT:$PC_{61}BM$ and PTB7:$PC_{71}BM$ in OPV cells. Iridium was used because it has a work function higher than that of ITO (4.5–4.8 eV) and lower than the HOMO level of the active layer (5.2 eV for P3HT and 6.1 eV PCBM). The results showed better performance of devices using metallic Ir as a surface modifier than FZTO/Ag/FZTO multilayer electrodes and iridium oxide-coated ITO electrodes. Therefore, iridium, as an efficient, chemically stable, and easy-to-manufacture surface modifier in devices, proves to be a very promising material for future organic electronic devices and therefore could be used as an alternative for PEDOT:PSS, which recently presented many disadvantages for the commercialization of BHJ solar cells.

Mutlu et al. (2019) [4] submitted titanium dioxide (TiO_2), which is the most widely used ETL in inverted OPV, to a process of immobilization of self-assembled parts in monolayers (SAM), intending to align energy levels between metal and semiconductor layers. The modification of TiO_2 (ETL) with different carboxylic acid-based SAMs such as C60, terthiophene, benzoic acid, and lauric acid can improve overall OPV performance compared to unmodified devices.

The recombination of charge carriers at the interface is reduced by passivation of surface trap states in TiO_2, which, together with the improved crystalline of the conjugated polymer P3HT, led to increased transfer of charge carriers. SAM molecules of 4′-[(3-methylphenyl)(phenyl)amino]biphenyl-4-carboxylic acid (device CT21) and bis[4-(hexyloxy)(phenyl)amino]biphenyl-4-carboxylic acid (CT23) were immobilized on the surface of the TiO_2 in the i-OPV structure. The effects of the inclusion of these monolayers were analyzed, and the results showed that the modification of the surface of the ETL layer resulted in the

improvement of the general photovoltaic parameters of solar cells. The main reason for this improvement, according to the authors, is that the working function of TiO_2 was adjusted with the insertion of the monolayer and with the modification of the molecular interface. Thus, the buffer layer's effective working function was altered by the chemical adsorption of SAM molecules on the surface of TiO_2. In addition, the dipolar strength of the CT23 monolayer was higher than that of the CT21 monolayer due to the hexyloxy chain, which has an electron donor group. Therefore, the TiO_2/CT23 electrode's effective working function was lower than the CT21-modified TiO_2 electrode [4].

7. Final Considerations

In addition to all the energy crises experienced in the 21st century, environmental consequences call for viable alternatives that can meet the needs of society. The photovoltaic technology containing polymers is a concrete alternative since it uses the most energetic renewable resource available, the sun. In addition, it enables the use and development of lightweight, flexible devices with ease of production and versatility in application.

The third-generation solar cells, especially OPV with polymers in the active layer, have the greatest potential for large-scale implementation, today the focus of a large field in photovoltaic research. Thus, it can be evidenced through this bibliographic survey that each type of conjugated polymers has its advantages, disadvantages, and great challenges to be overcome for future widespread commercialization. It is necessary to obtain high efficiency, stability, ease of production, reproducibility, and manufacturing process control. With thorough knowledge and mastery of parameters and variables, the OPV solar cells will have a competitive space in the world market.

Acknowledgments

The authors thank the Brazilian Council for Scientific and Technological Development (CNPq), the Coordination for the Improvement of Higher Education Personnel (CAPES), and the Carlos Chagas Filho Foundation for Supporting Research in the State of Rio de Janeiro (FAPERJ) for the financial support.

Conflict of interest

The authors declare no conflict of interest.

References

1. Ahmad KS, Naqvi SN, Jaffri SB (2021) Systematic review elucidating the generations and classifications of solar cells contributing towards environmental sustainability integration. *Rev Inorg Chem* 41: 21–39. https://doi.org/10.1515/revic-2020-0009
2. Sathiyan G, Siva G, Sivakumar EKT, et al. (2018) Synthesis and studies of carbazole-based donor polymer for organic solar cell applications. *Colloid Polym Sci* 296: 1193–1203. https://doi.org/10.1007/s00396-018-4337-4

3. Cui Y, Yao H, Gao B, et al. (2017) Fine-Tuned photoactive and interconnection layers for achieving over 13% efficiency in a fullerene-free tandem organic solar cell. *J Am Chem Soc* 139: 7302–7309. https://doi.org/10.1021/jacs.7b01493
4. Mutlu A, Can M, Tozlu C (2019) Performance improvement of organic solar cell via incorporation of donor type self-assembled interfacial monolayer. *Thin Solid Films* 685: 88–96. https://doi.org/10.1016/j.tsf.2019.05.064
5. Freudenberg J, Jänsch D, Hinkel F, et al. (2018) Immobilization strategies for organic semiconducting conjugated polymers. *Chem Rev* 118: 5598–5689. https://doi.org/10.1021/acs.chemrev.8b00063
6. Ragoussia M-E, Torres T (2015) New generation solar cells: Concepts, trends and perspectives. *Chem Commun* 51: 3957–3972. https://doi.org/10.1039/C4CC09888A
7. Majumder C, Rai A, Bose C (2018) Performance optimization of bulk heterojunction organic solar cell. *Optik* 157: 924–929. https://doi.org/10.1016/j.ijleo.2017.11.114
8. Chen S, Yang S, Sun H, et al. (2017) Enhanced interfacial electron transfer of inverted perovskite solar cells by introduction of CoSe into the electron-transporting-layer. *J Power Sources* 353: 123–130. https://doi.org/10.1016/j.jpowsour.2017.03.144
9. Mabindisa R, Tambwe K, Mciteka L, et al. (2021) Organic nanostructured materials for sustainable application in next generation solar cells. *Appl Sci* 11: 11324. https://doi.org/10.3390/app112311324
10. Oh Kwon K, Uddin MA, Park J-H, et al. (2016) A high efficiency nonfullerene organic solar cell with optimized crystalline organizations. *Adv Mater* 28: 910–916. https://doi.org/10.1002/adma.201504091
11. Li Z, Zhu C, Yuan J, et al. (2022) Optimizing side chains on different nitrogen aromatic rings achieving 17% efficiency for organic photovoltaics. *J Energy Chem* 65: 173–178. https://doi.org/10.1016/j.jechem.2021.05.041
12. Wibowo FTA, Krishna NV, Sinaga S, et al. (2021) High-efficiency organic solar cells prepared using a halogen-free solution process. *Cell Rep Phys Sci* 2: 100517. https://doi.org/10.1016/j.xcrp.2021.100517
13. Bi P, Zhang S, Chen Z, et al. (2021) Reduced non-radiative charge recombination enables organic photovoltaic cell approaching 19% efficiency. *Joule* 5: 2408–2419. https://doi.org/10.1016/j.joule.2021.06.020
14. Distler A, Brabec CJ, Egelhaaf H-J (2021) Organic photovoltaic modules with new world record efficiencies. *Prog Photovoltaics: Res Appl* 29: 24–31. https://doi.org/10.1002/pip.3336
15. Ma L, Zhang S, Wang J, et al. (2020) Recent advances in non-fullerene organic solar cells: from lab to fab. *Chem Commun* 56: 14337. https://doi.org/10.1039/D0CC05528J
16. Yao C, Zhao J, Zhu Y, et al. (2020) Trifluoromethyl Group-Modified Non-Fullerene acceptor toward improved power conversion efficiency over 13% in polymer solar cells. *ACS Appl Mater Interfaces* 12: 11543–11550. https://doi.org/10.1021/acsami.9b20544
17. Yang Y (2021) The original design principles of the Y-Series nonfullerene acceptors, from Y1 to Y6. *ACS Nano* 15: 18679–18682. https://doi.org/10.1021/acsnano.1c10365
18. Wagenpfahl A (2017) Mobility dependent recombination models for organic solar cells. *J Phys: Condens Matter* 29: 373001. https://doi.org/10.1088/1361-648X/aa7952

19. Xu B, Zheng Z, Zhao K, et al. (2016) A bifunctional interlayer material for modifying both the anode and cathode in highly efficient polymer solar cells. *Adv Mater* 28: 434–439. https://doi.org/10.1002/adma.201502989
20. Zheng Z, Hu Q, Zhang S, et al. (2018) A highly efficient non-fullerene organic solar cell with a fill factor over 0.80 enabled by a fine-tuned hole-transporting layer. *Adv Mater* 30: 1–9. https://doi.org/10.1002/adma.201801801
21. Doat O, Barboza BH, Batagin-Neto A, et al. (2021) Review: materials and modeling for organic photovoltaic devices. *Polym Int* 71: 6–25. https://doi.org/10.1002/pi.6280
22. Zhao Y, Zhu Y, Cheng H-W, et al. (2021) A review on semitransparent solar cells for agricultural application. *Mater Today Energy* 22: 100852. https://doi.org/10.1016/j.mtener.2021.100852
23. Bi P, Zhang S, Chen Z, et al. (2021) Reduced non-radiative charge recombination enables organic photovoltaic cell approaching 19% efficiency. *Joule* 5: 2408–2419. https://doi.org/10.1016/j.joule.2021.06.020
24. Zuo L, Shi X, Jo SB, et al. (2018) Tackling energy loss for high-efficiency organic solar cells with integrated multiple strategies. *Adv Mater* 30: 1706816. https://doi.org/10.1002/adma.201706816
25. Wilken S, Scheunemann D, Dahlström S, et al. (2021) How to reduce charge recombination in organic solar cells: There are still lessons to learn from P3HT:PCBM. *Adv Electron Mater* 7: 2001056. https://doi.org/10.1002/aelm.202001056
26. Nakano K, Terado K, Kaji Y, et al. (2021) Reduction of electric current loss by Aggregation-Induced molecular alignment of a Non-Fullerene acceptor in organic photovoltaics. *ACS Appl Mater Interfaces* 13: 60299–60305. https://doi.org/10.1021/acsami.1c19275
27. Pugliese SN, Gallaher JK, Uddin MA, et al. (2022) Spectroscopic comparison of charge dynamics in fullerene and non-fullerene acceptor-based organic photovoltaic cells. *J Mater Chem C*. https://doi.org/10.1039/D1TC04800G
28. Zhao F, Zhang H, Zhang R, et al. (2020) Emerging approaches in enhancing the efficiency and stability in Non-Fullerene organic solar cells. *Adv Energy Mater* 10: 2002746. https://doi.org/10.1002/aenm.202002746
29. Zhu L, Zhang M, Zhong W, et al. (2021) Progress and prospects of the morphology of non-fullerene acceptor based high-efficiency organic solar cells. *Energy Environ Sci* 1: 4341–4357. https://doi.org/10.1039/D1EE01220G
30. Lin Y, Zhao F, Wu Y, et al. (2016) Mapping polymer donors toward high-efficiency fullerene free organic solar cells. *Adv Mater* 29: 1604155. https://doi.org/10.1002/adma.201604155
31. Chung HY, Park J-H, Cui J, et al. (2021) Influence of intramolecular charge-transfer characteristics of excitons on polaron generation at the Donor/Acceptor interface in polymer solar cells. *J Phys Chem C* 125: 18352–18361. https://doi.org/10.1021/acs.jpcc.1c05524
32. Etxebarria I, Ajuria J, Pacios R (2015) Solution-processable polymeric solar cells: A review on materials, strategies and cell architectures to overcome 10%. *Org Electron: Phys, Mater, Appl* 19: 34–60. https://doi.org/10.1016/j.orgel.2015.01.014
33. Zuo L, Yu J, Shi X, et al. (2017) High-Efficiency nonfullerene organic solar cells with a parallel tandem configuration. *Adv Mater* 29: 1702547. https://doi.org/10.1002/adma.201702547
34. Zheng NN, Wang ZF, Zhang K, et al. (2019) High-performance inverted polymer solar cells without an electron extraction layer via a one-step coating of cathode buffer and active layer. *J Mater Chem A* 7: 1429–1434. https://doi.org/10.1039/c8ta09763a

35. Pandey R, Lim JW, Kim JH, et al. (2018) Performance enhancement in organic photovoltaic solar cells using iridium (Ir) ultra-thin surface modifier (USM). *Appl Surf Sci* 444: 97–104. https://doi.org/10.1016/j.apsusc.2018.03.012
36. Sun C, Pan F, Bin H, et al. (2018) A low cost and high performance polymer donor material for polymer solar cells. *Nature Commun* 9: 1–10. https://doi.org/10.1038/s41467-018-03207-x
37. Shen W, Xiao M, Tang J, et al. (2015) Effective regulation of the micro-structure of thick P3HT: PC 71 BM film by the incorporation of ethyl benzenecarboxylate in toluene solution. *RSC Adv* 5: 47451–47457. https://doi.org/10.1039/C5RA06957B
38. Wang D, Wright M, Elumalai NK, et al. (2016) Stability of perovskite solar cells. *Sol Energy Mater Sol Cells* 147: 255–275. https://doi.org/10.1016/j.solmat.2015.12.025
39. Salem AMS, El-Sheikh SM, Harraz FA, et al. (2017) Inverted polymer solar cell based on MEH-PPV/PC 61 BM coupled with ZnO nanoparticles as electron transport layer. *Appl Surf Sci* 425: 156–163. https://doi.org/10.1016/j.apsusc.2017.06.322
40. Ranganathan K, Wamwangi D, Coville NJ (2015) Plasmonic Ag nanoparticle interlayers for organic photovoltaic cells: An investigation of dielectric properties and light trapping. *Sol Energy* 118: 256–266. https://doi.org/10.1016/j.solener.2015.05.022
41. Meyer J, Hamwi S, Kröger M, et al. (2012) Transition metal oxides for organic electronics: Energetics, device physics and applications. *Adv Mater* 24: 5408–5427. https://doi.org/10.1002/adma.201201630
42. Nuramdhani I, Jose M, Samyn P, et al. (2019). Charge-Discharge characteristics of textile energy storage devices having different PEDOT:PSS ratios and conductive yarns configuration. *Polymers* 11: 345. https://doi.org/10.3390/polym11020345
43. Mota IC, Santos BPS, Santos REPD, et al. (2021) Influence of reaction time on properties of regioregular poly(3-hexylthiophene) by the Grignard metathesis polymerization. *J Therm Anal Calorim* 2021: 1–26. https://doi.org/10.1007/s10973-021-10890-4
44. Ghosekar IC, Patil GC (2021) Review on performance analysis of P3HT:PCBM based bulk heterojunction organic solar cells. *Semicond Sci Technol* 36: 045005. https://doi.org/10.1088/1361-6641/abe21b
45. Chen K-W, Lin L-Y, Li Y-H, et al. (2018) Fluorination effects of A-D-A-type small molecules on physical property and the performance of organic solar cell. *Org Electron: Phy, Mater, Appl* 52: 342–349. https://doi.org/10.1016/j.orgel.2017.11.021
46. Sathiyan G, Thangamuthu R, Sakthivel P (2016) Synthesis of carbazole-based copolymers containing carbazole-thiazolo[5,4-:D] thiazole groups with different dopants and their fluorescence and electrical conductivity applications. *RSC Adv* 6: 69196–69205. https://doi.org/10.1039/C6RA08888K
47. Wang C, Liu F, Chen QM, et al. (2021) Benzothiadiazole-based conjugated polymers for organic solar cells. *Chin J Polym Sci* 39: 525–536. https://doi.org/10.1007/s10118-021-2537-8
48. Zhong W, Xiao J, Sun S, et al. (2016) Wide bandgap dithienobenzodithiophene-based π-conjugated polymers consisting of fluorinated benzotriazole and benzothiadiazole for polymer solar cells. *J Mater Chem C* 4: 4719–4727. https://doi.org/10.1039/C6TC00271D
49. Zhao Q, Qu J, He F (2020) Chlorination: An effective strategy for high-performance organic solar cells. *Adv Sci* 7: 2000509. https://doi.org/10.1002/advs.202000509

50. Chen W, Wu Y, Yue Y, et al. (2015) Efficient and stable large-area perovskite solar cells with inorganic charge extraction layers. *Science* 350: 944–948. https://doi.org/10.1126/science.aad1015
51. Li M, Gao K, Wan X, et al. (2017) Solution-processed organic tandem solar cells with power conversion efficiencies >12%. *Nature Photonics* 11: 85–90. https://doi.org/10.1038/nphoton.2016.240
52. Jo JW, Jung JW, Jung EH, et al. (2015) Fluorination on both D and A units in D-A type conjugated copolymers based on difluorobithiophene and benzothiadiazole for highly efficient polymer solar cells. *Energy Environ Sci* 8: 2427–2434. https://doi.org/10.1039/C5EE00855G
53. Chao P, Johner N, Zhong Xi, et al. (2019) Chlorination strategy on polymer donors toward efficient solar conversions. *J Energy Chem* 39: 208–216. https://doi.org/10.1016/j.jechem.2019.04.002
54. Zhou J, Zhang B, Geng Y, et al. (2021) Gradual chlorination at different positions of D-π-A copolymers based on benzodithiophene and isoindigo for organic solar cells. *Mater Rep: Energy* 1: 100065. https://doi.org/10.1016/j.matre.2021.100065.
55. Dai T, Lei P, Zhang B, et al. (2021) Tricyclic or pentacyclic D units: Design of D−π–A-Type copolymers for high V_{OC} organic photovoltaic cells. *ACS Appl Mater Interfaces* 13: 30756–30765. https://doi.org/10.1021/acsami.1c08487
56. Yan T, Bin H, Sun C, et al. (2018) Effect of Thieno[3,2-b]thiophene π-bridge on photovoltaic performance of a D-A copolymer of alkoxy-benzodithiophene-alt-fluoro-benzotriazole. *Org Electron* 55: 106–111. https://doi.org/10.1016/j.orgel.2018.01.018
57. Bin H, Xiao L, Liu Y, et al. (2014) Effects of donor unit and p-Bridge on photovoltaic properties of D–A copolymers based on Benzo[1,2-b:4,5-c']-dithiophene-4,8-dione acceptor unit. *J Polym Sci Part A: Polym Chem* 52: 1929–1940. https://doi.org/10.1002/pola.27209
58. Akkuratov AV, Mühlbach S, Susarova DK, et al. (2017) Positive side of disorder: Statistical fluorene-carbazole-TTBTBTT terpolymers show improved optoelectronic and photovoltaic properties compared to the regioregular structures. *Sol Energy Mater Sol Cells* 160: 346–354. https://doi.org/10.1016/j.solmat.2016.10.039
59. Jiang X, Yang Y, Zhu J, et al. (2017) Constructing D–A copolymers based on thiophene-fused benzotriazole units containing different alkyl side-chains for non-fullerene polymer solar cells. *J Mater Chem C* 5: 8179–8186. https://doi.org/10.1039/C7TC02098H
60. Zhou P, Yang Y, Chen X, et al. (2017) Design of a thiophene-fused benzotriazole unit as an electron acceptor to build D–A copolymers for polymer solar cells. *J Mater Chem C* 5: 2951–2957. https://doi.org/10.1039/C7TC00083A
61. Jiang X, Wang J, Yang Y, et al. (2018) Fluorinated Thieno[2′,3′:4,5]benzo[1,2-d][1,2,3]triazole: New acceptor unit to construct polymer donors. *ACS Omega* 3: 13894–13901. https://doi.org/10.1021/acsomega.8b02053
62. Chang C, Li W, Guo X, et al. (2018) A narrow-bandgap donor polymer for highly efficient as-cast non-fullerene polymer solar cells with a high open circuit voltage. *Org Electron* 58: 82–87. https://doi.org/10.1016/j.orgel.2018.04.001
63. Sun C, Pan F, Bin H, et al. (2018) A low cost and high performance polymer donor material for polymer solar cells. *Nature Commun* 9: 1–10. https://doi.org/10.1038/s41467-018-03207-x
64. Fan B, Zhang D, Li M, et al. (2019) Achieving over 16% efficiency for single-junction organic solar cells. *Sci China Chem* 62: 746–752. https://doi.org/10.1007/s11426-019-9457-5

65. Xiong J, Jin K, Jiang Y, et al. (2019) Thiolactone copolymer donor gifts organic solar cells a 16.72% efficiency. *Sci Bull* 64: 1573–1576. https://doi.org/10.1016/j.scib.2019.10.002
66. Liu Q, Jiang Y, Jin K, et al. (2020) 18% Efficiency organic solar cells. *Sci Bull* 65: 272–275. https://doi.org/10.1016/j.scib.2020.01.001
67. Matsuo Y, Hatano J, Kuwabara T, et al. (2012) Fullerene acceptor for improving open-circuit voltage in inverted organic photovoltaic devices without accompanying decrease in short-circuit current density. *Appl Phys Lett*, 100. https://doi.org/10.1063/1.3683469
68. Zhao G, He Y, Li Y (2010) 6.5% Efficiency of polymer solar cells based on poly(3-hexylthiophene) and Indene-C60 bisadduct by device optimization. *Adv Mater* 22: 4355–4358. https://doi.org/10.1002/adma.201001339
69. Cai Y, Li Y, Wang R, et al. (2021) A Well-Mixed phase formed by two compatible Non-Fullerene acceptors enables ternary organic solar cells with efficiency over 18.6%. *Adv Mater* 33: 2101733. https://doi.org/10.1002/adma.202101733
70. Li M, Gao K, Wan X, et al. (2017) Solution-processed organic tandem solar cells with power conversion efficiencies >12%. *Nature Photonics* 11: 85–90. https://doi.org/10.1038/nphoton.2016.240
71. Chen X, Kan B, Kan Y, et al. (2020) As-Cast ternary organic solar cells based on an asymmetric Side-Chains featured acceptor with reduced voltage loss and 14.0% efficiency. *Adv Funct Mater* 30: 1909535. https://doi.org/10.1002/adfm.201909535
72. Xiao L, Wu X, Ren G, et al. (2021) Highly efficient ternary solar cells with efficient förster resonance energy transfer for simultaneously enhanced photovoltaic parameters. *Adv Funct Mater* 31: 2105304. https://doi.org/10.1002/adfm.202105304
73. Sharma R, Lee H, Seifrid M, et al. (2020) Performance enhancement of conjugated polymer-small molecule-non fullerene ternary organic solar cells by tuning recombination kinetics and molecular ordering. *Sol Energy* 201: 499–507. https://doi.org/10.1016/j.solener.2020.03.008
74. Wan J, Zhang L, He Q, et al. (2020) High-Performance pseudoplanar heterojunction ternary organic solar cells with nonfullerene alloyed acceptor. *Adv Funct Mater* 30: 1909760. https://doi.org/10.1002/adfm.201909760
75. Liu T, Guo Y, Yi Y, et al. (2016) Ternary organic solar cells based on two compatible nonfullerene acceptors with power conversion efficiency >10%. *Adv Mater* 28: 10008–10015. https://doi.org/10.1002/adma.201602570
76. Kumari T, Lee SM, Yang C (2018) Cubic-Like bimolecular crystal evolution and over 12% efficiency in halogen-free ternary solar cells. *Adv Funct Mater* 28: 1707278. https://doi.org/10.1002/adfm.201707278
77. Xie L, Yang C, Zhou R, et al. (2020) Ternary organic solar cells BasedonTwoNon-fullerene acceptors with complimentary absorption and balanced crystallinity. *Chin J Chem* 38: 935–940. https://doi.org/10.1002/cjoc.201900554 (2020)
78. Xu R, Zhang K, Liu X, et al. (2018) Alkali Salt-Doped highly transparent and Thickness-Insensitive Electron-Transport layer for High-Performance polymer solar cell. *ACS Appl Mater Interfaces* 10: 1939–1947. https://doi.org/10.1021/acsami.7b17076
79. Singh A, Dey A, Das D, et al. (2016) Effect of dual cathode buffer layer on the charge carrier dynamics of rrP3HT: PCBM based bulk heterojunction solar cell. *ACS Appl Mater Interfaces* 8: 10904–10910. https://doi.org/10.1021/acsami.6b03102

80. Kageyama H, Kajii H, Ohmori Y, et al. (2011) MoO_3 as a cathode buffer layer material for the improvement of planar pn-heterojunction organic solar cell performance. *Appl Phys Express* 4: 032301. https://doi.org/10.1143/APEX.4.032301
81. Sachdeva S, Kaur J, Sharma K, et al. (2018) Performance improvements of organic solar cell using dual cathode buffer layers. *Curr Appl Phys* 18: 1592–1599. https://doi.org/10.1016/j.cap.2018.10.009
82. Yu X, Yu X, Zhang J, et al. (2015) Gradient Al-doped ZnO multi-buffer layers: Effect on the photovoltaic properties of organic solar cells. *Mater Lett* 161: 624–627. https://doi.org/10.1016/j.matlet.2015.09.017
83. Pandey R, Lim JW, Kim JH, et al. (2018) Performance enhancement in organic photovoltaic solar cells using iridium (Ir) ultra-thin surface modifier (USM). *Appl Surf Sci* 444: 97–104. https://doi.org/10.1016/j.apsusc.2018.03.012

AIMS Press